Available online at www.sciencedirect.com

ScienceDirect

Procedia Structural Integrity 7 (2017) 505–512

Structural Integrity Procedia

www.elsevier.com/locate/procedia

3rd International Symposium on Fatigue Design and Material Defects, FDMD 2017, 19-22 September 2017, Lecco, Italy

Effects of microstructure and casting defects on the fatigue behavior of the high-pressure die-cast AlSi9Cu3(Fe) alloy

L. Lattanzi[a]*, A. Fabrizi[b], A. Fortini[a], M. Merlin[a], G. Timelli[b]

[a]*University of Ferrara, Department of Engineering, Via Saragat 1, Ferrara 44122, Italy*
[b]*University of Padua, Department of Management and Engineering, Stradella San Nicola 3, Vicenza 36100, Italy*

Abstract

High-pressure die-cast (HPDC) components are being increasingly used due to good flexibility and high productivity. These aspects make HPDC suitable to produce several mass components, especially for the automotive sector. Due to the rapid filling of the die and high cooling rate, the process generally leads to the formation of a wide variety of defects, such as porosity and oxide films. Such defects might act as starting points for fatigue cracks and thus deteriorating the fatigue behavior of the casting. To this respect, the fatigue behavior of die cast aluminum alloys is an important aspect to consider when assessing the performance of complex castings for automotive applications. In the light of these aspects, the goal of this work is to describe how the microstructure affects the fatigue crack initiation and propagation. Die cast AlSi9Cu3(Fe) specimens were produced by means of a specifically designed die and the microstructure was preliminary characterized. Uniaxial fatigue tests were performed at load control with a stress ratio of R = 0.1 and at a single level of stress amplitude. After the fatigue tests, the samples were investigated to assess the propagation of the fatigue cracks; the starting points of cracks were specifically identified and the obtained data suggested how defects strongly influence the damage mechanism of the material.

Keywords: die cast aluminum alloy; casting defects; microstructure.

* Corresponding author. Tel.: +39-0532-974843.
E-mail address: lucia.lattanzi@unife.it

10.1016/j.prostr.2017.11.119

1. Introduction

In recent years, the fatigue behavior of die cast aluminum alloys has become of interest because of their increasing use in the automotive industry. High-pressure die-casting is characterized by good flexibility and high production speed, which are key features for the massive production of automotive components with complex geometry and good surface quality. The main drawback of the HPDC concerns the formation of a wide variety of casting defects, such as gas porosity, oxide films, and cold joints, as defined by PD CEN/TR 16749:2014 standard and proposed by Fiorese et al. 2015. These defects are known to affect the mechanical properties to some extent. Previous studies have reported that the influence of various casting defects on static strength appears to be different in each case, while important variations are observed for the elongation at rupture. Avalle et al. 2002 reported that the static characteristics of high-pressure die-cast AlSi9Cu3(Fe) specimens decrease by increasing the porosity level.

To date, the static mechanical properties of die cast Al alloy components have been extensively investigated, however very few studies have examined the role of high pressure die casting defects on the fatigue properties (Avalle et al. 2002, Mayer et al. 2003, Hu et al. 2014). Avalle et al. 2002 run fatigue tests on standard specimens in as die-cast conditions and on production components, and concluded that a combination of pores and cold joints determines a fatigue strength decrease. Mayer et al. 2003 compared the fatigue properties of cast Mg alloys with AlSi9Cu3(Fe) cast Al alloy, all produced similarly by high-pressure die-casting. The authors reported that in 98.5 % of specimens the crack initiates in correspondence of porosities and that all the investigated alloys showed a pronounced fatigue limit. Hu et al. 2014 conducted a systematic research on fatigue behavior of the AlMg5Si2Mn alloy produced by both permanent mold and HPDC. About the dynamic mechanical properties, the authors declared that fatigue limits of permanent mold specimens are shorter than that of high pressure die casting ones.

Several similar studies have been conducted about the cast defects influence on fatigue properties, but concerned sand casting (Wang et al. 2001), permanent mold casting (Serrano-Munoz et al. 2016, Mu et al. 2014) and low pressure die casting (Ammar et al. 2008). The conclusions are that the fatigue strength of materials containing defects is lower than that of the defect-free ones, and the size of a defect and its distance from a free surface determines the specimen fatigue life. In these investigations, the influence of casting defects on the fatigue behavior of cast aluminum alloys has been studied by means of fracture surface analysis and metallographic characterization.

In the light of these aspects, the purpose of this preliminary study is to better describe how the microstructure interacts with fatigue crack initiation and propagation in high-pressure die-cast AlSi9Cu3(Fe) aluminum alloy. The microstructural characterization was preliminary carried out by means of metallographic techniques. Load control fatigue tests were run on three specimens at a single load level and, after failure, the fracture surface and profile were investigated in detail with the aim of identifying the crack initiation site and studying the role of defects on the fatigue failure.

2. Experimental procedure

2.1. Alloy and die casting parameters

Die cast AlSi9Cu3(Fe) (EN AC-46000) alloy, whose composition is reported in Table 1, was used to produce specimens by a cold-chamber die casting machine with a locking force of 2.9 MN. Oil circulation channels in the die were used to stabilize the temperature (at ~230 °C), while the fill fraction of the shot chamber was 0.28. The plunger velocity was 0.2 $m \cdot s^{-1}$ for the first phase and 2.7 $m \cdot s^{-1}$ for the filling phase; the intensification pressure was 40 MPa.

Table 1. The chemical composition of the experimental alloy (wt.%).

Cu	Mg	Si	Fe	Mn	Ni	Zn	Cr	Al
2.825	0.252	8.227	0.799	0.261	0.081	0.895	0.083	bal.

The multi-specimen casting depicted in Fig. 1, composed of specimens for different mechanical tests, was produced by a specifically designed die. The weight of the Al alloy die casting was 0.9 kg, including runners, gating and overflow system.

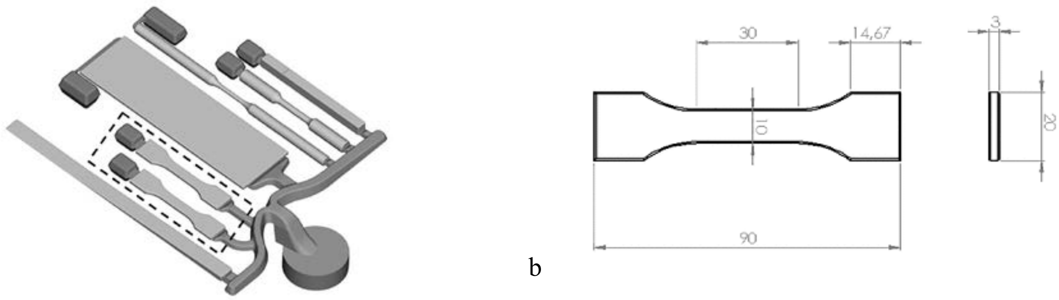

a b

Fig. 1. (a) Geometry of the die casting, the investigated specimens are indicated by the dashed line rectangle; (b) technical design of the tensile specimen.

In the present study, the flat specimens with a nominal thickness of 3 mm underwent uniaxial fatigue tests. The gauge length and width are 35 and 10 mm, respectively. The average static tensile properties of these specimens in terms of yield strength, ultimate tensile strength and elongation to fracture are 165 MPa, 315 MPa, and 4 %, respectively (Timelli et al. 2011).

2.2. Fatigue tests

Before being tested, the as die-cast components were stored at room temperature for several years and consequently were in a T1 condition, i.e. cooling from the casting temperature and natural aging. Uniaxial fatigue tests were performed on LM10 Italsigma testing machine, powered by linear electric motors, at load control with a frequency of 50 s^{-1} and with a stress amplitude of 80 MPa. A stress ratio of R = 0.1, which corresponds to a tension-tension cycle with $\sigma_{min}=0.1\cdot\sigma_{max}$, was applied. This stress cycle leads to severe conditions since consists exclusively in traction loads. For this reason, it is often used in automotive and aircraft component testing, as stated by Roylance 2001.

2.3. Microstructural investigations

Preliminary microstructural investigations were performed on some specimens by means of different techniques. In particular, microstructural observations were carried out by means of optical (OM) and scanning electron microscopy (SEM), while the identification of the phases was performed by X-ray diffraction (XRD) technique. Moreover, the evaluation of the grain size and texture was performed by electron back-scattered diffraction (EBSD) investigations. After fatigue testing, the fracture surface and profile were studied to evaluate the crack initiation and propagation by both optical and scanning electron microscopy.

3. Results and discussion

3.1. General microstructure

The typical microstructure of the alloy near the surface is shown in Fig. 2a and Fig. 2b depicts the microstructure at the center of the specimen. It is worth noting that the difference between the observed microstructures is due to different cooling rates that occur on the surface and in the center. The α-Al dendrites are not developed in length and show a rosette-like morphology, which is typical of a globular grain structure where the grain size is comparable with SDAS values.

The grain structure was further investigated at the center of the cross-section of the specimens and the distribution of grain size is plotted in Fig. 3a. The equiaxed grains are size-distributed according to a three-parameters log-normal distribution. The average values of grain size (*d*) and secondary dendrite arm spacing (SDAS) at the core region of the samples are very similar, as shown in Table 2.

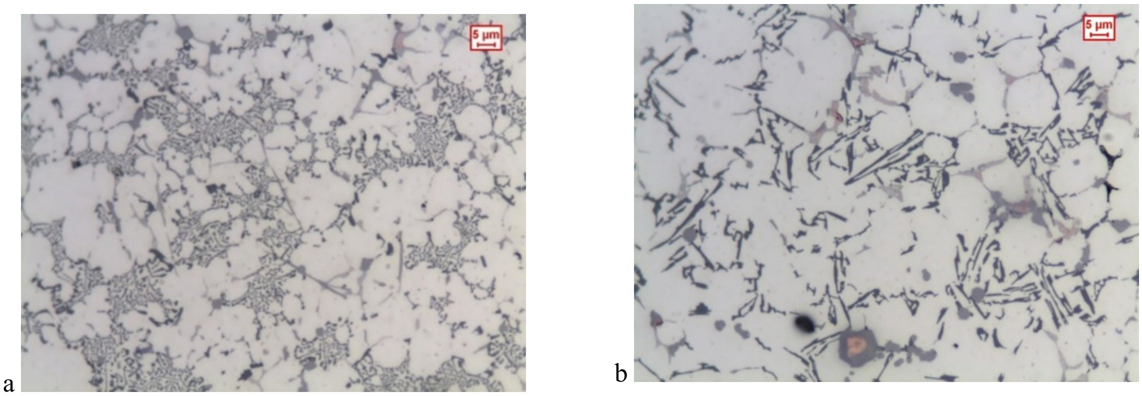

Fig. 2. Typical OM micrograph of a specimen: (a) near the surface; (b) at the center.

Table 2. Average values of grain size and secondary dendrite arm spacing at the center of the specimen cross-section.

Microstructural parameter	Average dimension [µm]
Grain size	17 ± 8
SDAS	12 ± 2

The d/SDAS ratio results lower than 1.6: when this value is less than 2, the grain morphology is spherical or globular. This result confirms the previous observations of OM micrographs. The analysis of the polar figure reported in Fig. 3b shows that there is no evidence of a preferential orientation of the grain structure.

In order to reveal and identify the intermetallic phases in the examined alloy, EDS spectra and elemental maps were performed and the results were presented in previous works (Fabrizi et al. 2013). Acicular Fe-rich compounds were identified as β-Al_5FeSi phase. The XRD spectrum in Fig. 4a confirmed the presence of more frequent intermetallic compounds such as θ-Al_2Cu and blocky α-Al(Fe,Mn,Cr)Si (*sludge*) phases. A SEM micrograph indicating the latter intermetallic compounds is depicted in Fig. 4b.

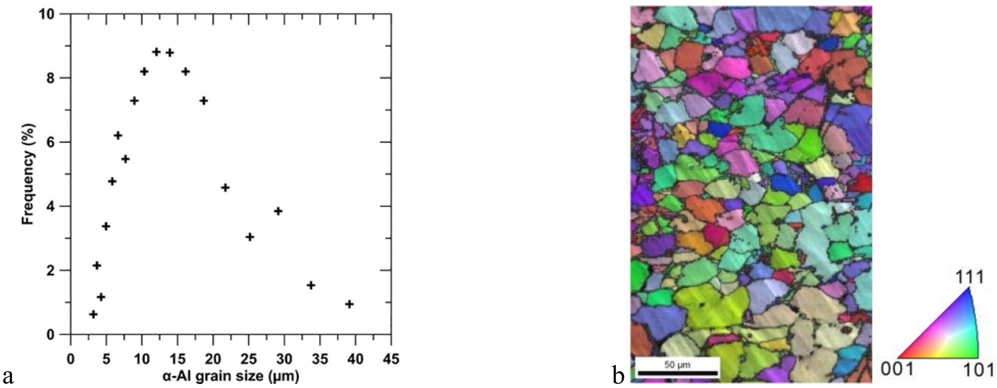

Fig. 3. (a) α-Al grain size dimension distribution; (b) EBSD orientation map obtained in the central cross-section of the specimen.

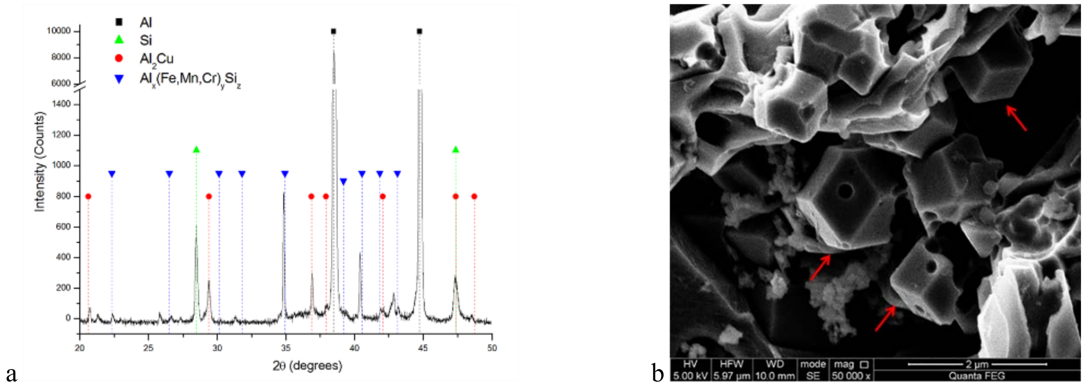

Fig. 4. Analyses of secondary phases: (a) XRD spectrum; (b) SEM micrograph of blocky sludge phases.

Typical microstructure of the specimen cross section is shown in Fig. 5 and is possible to distinguish networks of intermetallic compounds, that are larger than the ones observed close to the casting surfaces. This characteristic is due to the higher undercooling at the die wall so that nucleation prevails on the growing mechanism. Timelli et al. 2011 highlighted a significant eutectic segregation band by means of OM observations on the fluidity appendix cross-section, as can be seen in Fig. 6a.

The presence of this segregation band indicates a positive macro-segregation, i.e. a localized enrichment of Al-Si eutectic, and can form during the second or third phases of the process, i.e. the filling phase and the compacting phase respectively. In addition, as depicted in Fig. 6b, a concentration of gas porosity at the center of the region delimited by the segregation band was found on the cross-section of the tensile specimen.

Considering the results of the microstructural analysis, despite the equiaxial grain structure and the absence of a preferential texture, the presence of an evident segregation band and gas porosities induced by the specific process could strongly affect the dynamic mechanical properties of the alloy.

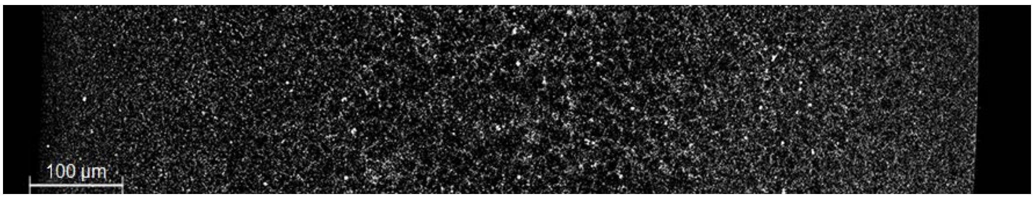

Fig. 5. SEM image of the specimen cross-section.

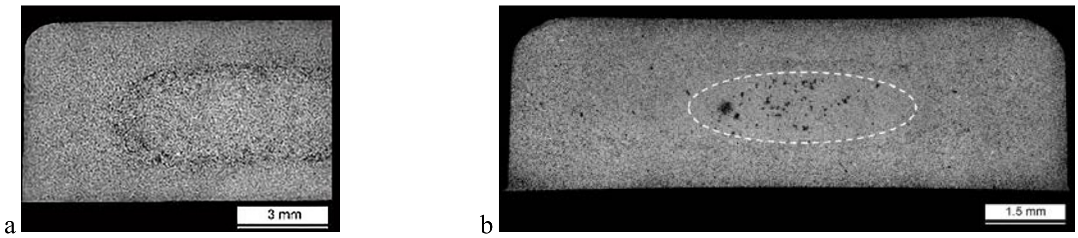

Fig. 6. (a) eutectic segregation region in the specimen cross-section; (b) porosity in the tensile specimen cross-section.

3.2. Fatigue tests and fracture investigations

Fatigue life of die-cast specimens is above 4×10^4 cycles under the stress level of 80 MPa. In particular, specimens failed at 8.7×10^4 cycles, 4.4×10^4 cycles, and 10×10^4 cycles. The observed data scatter indicates that the fatigue life should strongly depend on the presence of die-cast defects. It should be noted that the specimens were consecutively die-cast and fatigue tests were performed with the same sequence.

The fatigue fracture surfaces of the specimens were examined with scanning electron microscopy to identify the crack initiation sites and the propagation areas. Fig. 7a shows the initiation region of the specimen that failed at 8.7×10^4 cycles. The fatigue cracks initiate at one of the section sharp corners in all the specimens evaluated. In addition, it seems that the crack initiated and propagated from a single site.

Two different regions can be distinguished on the fracture surface: a limited bright area adjacent to the initiation site and an irregular surface region that includes the remaining specimen section. This area distinction is similar to the one reported by Ammar et al. 2008 and Mu et al. 2014 for circular cross-section specimens. The bright area corresponds to the stable fatigue crack propagation phase, while the rugged region far from the initiation site refers to the final static fracture. The initiation site is identified with the convergence of the propagation rivers. The width of the bright regular area is limited with respect to the rest of specimen surface and has a radius between 1.5 and 2 mm (from 50 % to 67 % of the specimen thickness). It was observed that the fracture occurred because of the presence of oxide films and cold joints in correspondence of the section corner, as can be seen in Fig. 7b for the specimen that failed at 8.7×10^4 cycles. Avalle et al. found similar alumina skins and cold joints on the fracture surfaces as initiation sites. These defects cause a discontinuity in the material and fatigue fractures can easily initiate.

On the irregular region both sludge particles and gas porosities, previously observed in the center of the cross-section, can be distinguished in Fig. 8a and Fig. 8b.

The fracture profile was investigated by optical microscopy and the transition zone from the regular area to the irregular one was identified. Fig. 9a shows the profile micrograph of the specimen that failed at 8.7×10^4 cycles, representative of the others. From the initiation point, the profile is smooth and regular and corresponds to the bright area observed on the fracture surface (Fig. 9b). After the transition zone the profile becomes rough and irregular (Fig. 9c), reflects the rugged surface observed in SEM micrographs and represents the sudden failure of the specimen.

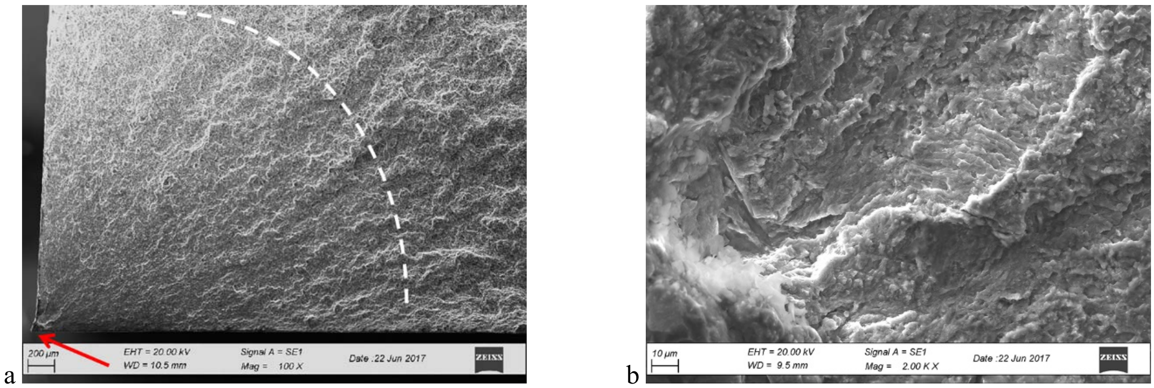

Figure 7. SEM images of the specimen that failed at 8.7×10^4 cycles: (a) crack initiation region. The red arrow indicates the crack initiation site while the dashed line highlights the transition region; (b) particular of the crack origin site.

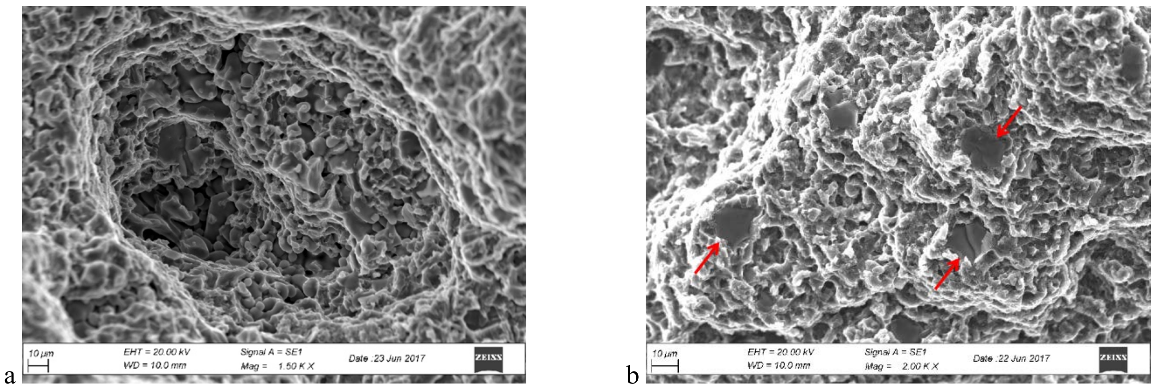

Figure 8. SEM images of surface features: (a) gas porosity; (b) fractured sludge particles.

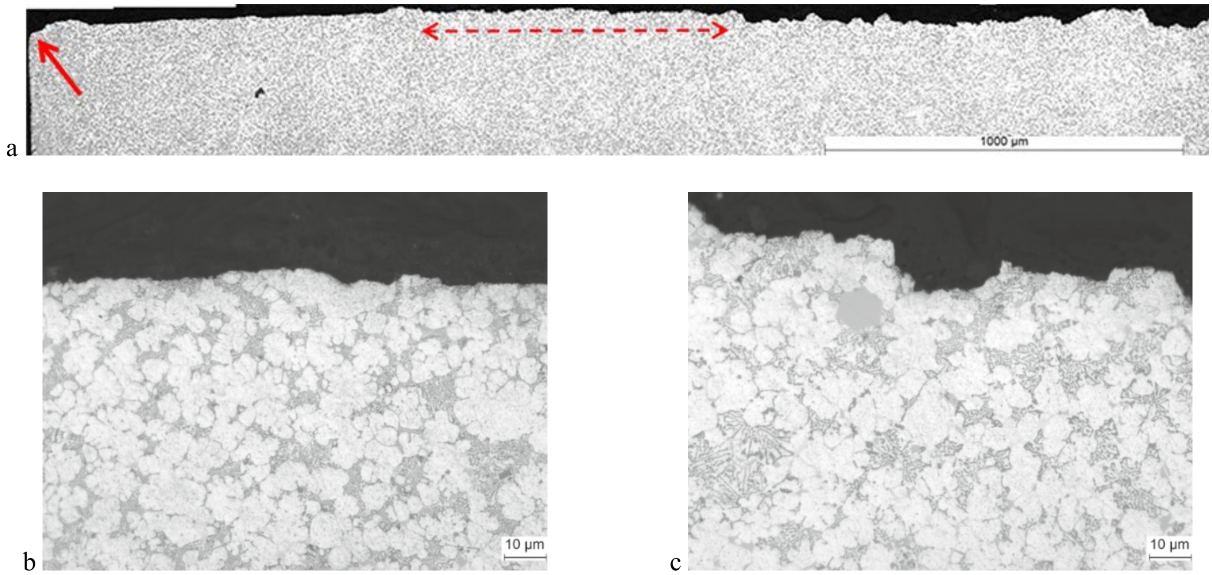

Fig. 9. Fracture profile of the specimen that failed at 8.7×10^4 cycles. (a) the red arrow indicates the crack initiation point and the dashed arrow indicates the transition region; (b) crack propagation region at high magnification; (c) static failure region at high magnification.

The fracture path proceeds both in the interdendritic eutectic region and also crosses the dendrites during the initial propagation phase as depicted in Fig. 9b. Conversely, during the static failure (Fig. 9c) the fracture line follows the dendritic structure profile. This characteristic is due to the failure of the interdendritic constituents, i.e. silicon eutectic particles and Fe-rich intermetallics, that promote the fracture propagation.

4. Conclusions

Uniaxial fatigue tests with load ratio of R=0.1 have been performed on high-pressure die-cast EN AC 46000 specimens. Preliminary investigations were performed in order to identify the microstructural constituents. Fracture surfaces and profiles were investigated by means of OM and SEM. According to the findings, the following observations can be drawn:

- The presence of a segregation band has been detected and indicates a positive macro-segregation. Moreover, a concentration of gas porosity at the center of the region delimited by the segregation band was found.
- Fatigue fracture occurred at a different number of cycles for the three specimens. The data scatter implies that defects control crack propagation, thus influence the specimen fatigue behavior, while crack initiation seems to be influenced by geometrical characteristics.
- In the considered specimens, cracks were initiated near oxide films and cold joints, typical casting defects in die castings. These defects are located in the sharp corner of the specimen cross-section possibly due to the convergence at the corner of different cold and warm metal flows.
- The fracture surface consists of a limited stable propagation area, with a regular evolution, and an extended static fracture region. Sludge particles and gas porosities can be observed on the irregular area of the surface.
- The fracture profile analysis was also used to distinguish both the smooth and rugged portions of the fatigue crack path.

This preliminary study will be deepened in order to investigate the role of microstructural constituents. Moreover, a higher number of fatigue tests will be performed in order to enable a statistical evaluation of the defects influence on the number of cycles to failure.

Acknowledgements

The authors would like to thank Ing. Roberto Ravegnani and Ing. Franco Giuliani of Italsigma for helping with the fatigue tests.

References

Ammar H.R., Samuel A.M., Samuel F.H., 2008. Porosity and the fatigue behavior of hypoeutectic and hypereutectic aluminum-silicon casting alloys. International Journal of Fatigue 30, 1024-1035.

Avalle M., Belingardi G., Cavatorta M.P., Doglione R., 2002. Casting defects and fatigue strength of a die cast aluminium alloy: a comparison between standard specimens and production components. International Journal of Fatigue 24, 1-9.

Fabrizi A., Ferraro S., Timelli G., 2013. The influence of Sr, Mg and Cu addition on the microstructural properties of a secondary AlSiCu3(Fe) die casting alloy. Materials Characterization 85, 13-25.

Fiorese E., Bonollo F., Timelli G., Arnberg L., Gariboldi E., 2015. New classificationof defects and imperfections for aluminum alloy castings. International Journal of Metalcasting 9, 55-66.

Hu Z., Wan L., Lu S., Zhu P., Wu S., 2014. Research on the microstructure, fatigue and corrosion behavior of permanent mold and die cast aluminum alloy. Materials and Design 55, 353-360.

Mayer H., Papakyriacou M., Zettl B., Stanzl-Tschegg S.E., 2003. Influence of porosity on the fatigue limit of die cast magnesium and aluminium alloys. International Journal of Fatigue 25, 245-256.

Meneghetti G., Susmel L., Tovo R., 2007. High-cycle fatigue crack paths in specimens having different stress concentration features. Engineering Failure Analysis 14, 656-672.

Mu P., Nadot Y., Nadot-Martin C., Chabod A., Serrano-Munoz I., Verdu C., 2014. Influence of casting defects on the fatigue behavior of cast aluminum AS7G06-T6. International Journal of Fatigue 63, 97-109.

Serrano-Munoz I., Buffiere J.-Y., Verdu C., Gaillard Y., Mu P., Nadot Y., 2016. Influence of surface and internal casting defects on the fatigue behaviour of A357-T6 cast aluminium alloy. International Journal of Fatigue 82, 361-370.

Timelli G., Ferraro S., Grosselle F., Bonollo F., Voltazza F., Capra L., 2011. Caratterizzazione meccanica e microstrutturale di leghe di alluminio pressocolate. La Metallurgia Italiana 1, 5-17.

Wang Q.G., Apelian D., Lados D.A., 2001. Fatigue behavior of A356-T6 aluminum cast alloys. Part I. Effect of casting defects. Journal of Light Metals 1, 73-84.